The Molecular Behavior of 1,3,5-Trioxane in a Cyclophosphazene Inclusion Compound: A ^{2}H NMR Study

Ansgar Liebelt,[†] Andreas Detken,[‡,§] and Klaus Müller*[,†]

Institut für Physikalische Chemie, Universität Stuttgart, Pfaffenwaldring 55, D-70569 Stuttgart, Germany, and Max-Planck-Institut für Medizinische Forschung, Jahnstrasse 29, D-69120 Heidelberg, Germany

Received: April 2, 2002

Dynamic ^{2}H NMR techniques were employed to examine the ordering behavior and dynamics of perdeuterated 1,3,5-trioxane-d_6 in the inclusion compound with tris-(1,2-dioxyphenyl)-cyclotriphosphazene. The experimental data, obtained by variable-temperature line shape studies, spin−spin and spin−lattice relaxation, and 2D exchange experiments between 30 and 370 K, were analyzed in a quantitative way by carrying out theoretical calculations on the basis of various motional models. At room temperature, highly mobile trioxane guests are observed. They undergo various overall and conformational motions that give rise to a substantial orientational disorder within the hexagonal cyclophosphazene channels. For the present inclusion compound, the following guest motions could be assigned: (i) molecular rotation about the molecular C_3-axis of the guests (rotational diffusion process), (ii) rotation about the host channel symmetry axis (3-fold jump process), (iii) overall fluctuation, and (iv) ring inversion. It could be shown that the two symmetry axes for rotational motions are oriented perpendicular to each other, that is, the C_3-axes of the trioxane guests are inclined at an angle of 90° with respect to the channel long axis. The activation energies for the overall rotations were found to be rather low with values of 10.0 and 10.9 kJ/mol for the motion about the C_3-axis and channel long axis, respectively. For the ring inversion process, an activation energy of 50.0 kJ/mol was derived that is almost identical with the values reported from previous solution NMR studies.

Introduction

Inclusion compounds are interesting materials for several reasons.[1,2] On one hand, they are of interest in applied chemistry. For instance, they possess high selectivity with respect to the guest upon enclathration and can be used for directed synthesis. On the other hand, inclusion compounds can serve as model systems for the study of molecules under confined conditions. Hence, the study of such systems can provide additional information about the molecular interactions between the various components in such guest−host complexes.

In the past, various experimental techniques, such as X-ray crystallography, differential scanning calorimetry, or NMR spectroscopy, were applied that primarily were addressed to the static properties of inclusion compounds.[1,2] More recently, the interest also turned toward the dynamic features of these systems. For instance, it could be shown that in such solid complexes highly mobile guest molecules may exist.[3] In this context, NMR spectroscopy has proven to be a reliable technique to sort out the molecular behavior of these inherently dynamic systems. Variable-temperature ^{2}H NMR techniques, also successfully employed during the study of other chemical systems,[4−7] turned out to be of particular help. From the analysis of ^{2}H NMR line shapes, relaxation data, and 2D exchange NMR experiments, a large dynamic range (up to about 10 orders of magnitude), not accessible with any other experimental technique, could be covered.

Inclusion compounds can be formed by various types of organic or inorganic compounds. Among these, thiourea and urea are well-known host components. In the presence of suitable guest compounds, they build up hexagonal channels, in which the guest species are incorporated.[1,2] Urea and thiourea inclusion compounds primarily are distinguished by their channel diameters,[8] which are the main criterion for the selectivity of the enclathrated guests. Thus, elongated molecules, such as *n*-alkanes, are enclathrated in the urea channels, while thiourea channels show a preference toward bulkier guests, such as cycloalkanes. Numerous studies have been published on such urea or thiourea systems dealing with the static properties of mainly the host lattice, as well as the dynamic features of the guest components.[3,9]

Further host compounds of increasing interest are cyclophosphazene derivatives.[10−12] In contrast to the above-mentioned urea or thiourea hosts, cyclophosphazenes turned out to be less-selective with respect to the enclathrated guests. Thus, cyclophosphazene inclusion compounds with guest molecules of quite different chemical structures, such as benzene, benzene derivatives, cycloalkanes, or *n*-alkanes, can be prepared. So far, only a few X-ray studies for cyclophosphazene inclusion compounds are known.[13,14] They showed that the host lattice—in analogy to the urea and thiourea inclusion compounds—is characterized by hexagonal channels. Likewise, ^{2}H NMR studies have been published on cyclophosphazene inclusion compounds with benzene and related compounds, which again revealed a high mobility of such guest molecules in the cyclophosphazene channels.[15−18]

We have recently started to study the behavior of various saturated six-membered guests in cyclophosphazene inclusion compounds.[19] These investigations are addressed to the exami-

* To whom correspondence should be addressed. Phone: (++49) 711 685 4470. Fax: (++49) 711 685 4467. E-mail: k.mueller@ipc.uni-stuttgart.de.

[†] Universität Stuttgart.

[‡] Max-Planck-Institut für Medizinische Forschung.

[§] Present address: Laboratorium für Physikalische Chemie, ETH-Zentrum, Universitätsstrasse 22, CH-8092 Zürich, Switzerland.

10.1021/jp025879e CCC: $22.00
Published on Web 07/20/2002

nation of the ordering and motional characteristics of the guest species and their dependence on the particular molecular structure of these guests. In this contribution, we report on a comprehensive ^{2}H NMR study of the inclusion compound from tris-(1,2-dioxyphenyl)-cyclotriphosphazene (in the following simply denoted as cyclophosphazene) with perdeuterated 1,3,5-trioxane-d_6. The analysis of the variable-temperature ^{2}H NMR experiments—comprising line shape, relaxation measurements, and 2D exchange experiments—was done on the basis of appropriate motional models, from which a detailed picture about the molecular features of the guest components could be achieved. It is shown that several thermally activated guest motions exist that give rise to a substantial motional and thus orientational disorder at elevated temperatures. Furthermore, the analysis of the variable-temperature experiments provides the kinetic parameters of the assigned guest motions. These quantities describing the guest dynamics along with the results for the ordering behavior are discussed and contrasted with the known data for related systems.

Experimental Section

Materials. All chemicals used during the synthetic work were obtained from Aldrich Chemicals. Perdeuterated 1,3,5-trioxane-d_6 was prepared by heating a solution of deuterated paraformaldehyde $(CD_2O)_x$ in D_2O and concentrated (98%) D_2SO_4, as described elsewhere.[20] The pure 1,3,5-trioxane-d_6 was obtained via repeated sublimation of the crude material. Tris-(1,2-dioxyphenyl)-cyclotriphosphazene was synthesized by the reaction of hexachlorocyclotriphosphazene with catechol in the presence of Na_2CO_3 in tetrahydrofuran. The crude product was purified by subsequent washing with diluted HCl and distilled water, followed by vacuum sublimation. Further details can be found elsewhere.[12,21]

Inclusion compounds of tris-(1,2-dioxyphenyl)-cyclotriphosphazene with 1,3,5-trioxane-d_6 were obtained after strirring a mixture of both components in chloroform.[12] The solvent was removed in a vacuum. The quality of the inclusion compound was checked by ^{13}C MAS NMR spectroscopy. For the sample used in the present ^{2}H NMR work, only the ^{13}C resonances of the guest and the host components were detectable. The guest-to-host ratio was found to be approximately 1:2.

NMR Measurements. ^{2}H NMR measurements above 90 K were performed on a Bruker CXP 300 spectrometer (Bruker/Rheinstetten) operating at a frequency of 46.07 MHz for deuterium, equipped with a Tecmag control unit (Tecmag/Houston). For the low-temperature ^{2}H NMR experiments ($T <$ 90 K), a home-built NMR spectrometer at the Max-Planck-Institut/Heidelberg (^{2}H frequency 72.1 MHz) equipped with a liquid-helium flow cryostat (Oxford instruments) was used. All measurements were done with home-built 5 mm NMR probes and $\pi/2$ pulse widths of 2.7 μs (46.07 MHz spectrometer) or 2.0 μs (72.1 MHz spectrometer). ^{2}H NMR spectra were recorded using the quadrupole echo sequence $[(\pi/2)_x-\tau_e-(\pi/2)_y-\tau_e-$acq] and a time interval between the pulses of $\tau_e = 20$ μs. Partially (T_2) relaxed ^{2}H NMR spectra, as well as spin−spin relaxation times, were obtained with the same pulse sequence by changing the interval τ_e between the $\pi/2$ pulses. For the determination of the spin−lattice relaxation times and the corresponding partially relaxed spectra, a modified version of the inversion recovery sequence $[\pi-\tau_r-(\pi/2)_x-\Delta-(\pi/2)_y-\Delta-$acq] with a constant value of $\Delta = 20$ μs was used. Here, the π-pulse was replaced by a composite pulse—$(\pi/2)_\phi(\pi/2)_{\phi\pm\pi/2}$-$(\pi/2)_\phi$ (phase cycling $\phi = 0, \pi/2, \pi, 3\pi/2$)—to ensure complete spectrum inversion.[22] The number of scans in these experiments varied between 256 and 1024. For the deuterium 2D exchange NMR spectra, two separate data sets from spin alignment echo and stimulated echo experiments were recorded. Both experiments are based on a four-pulse sequence $[(90°)_{\phi_1}-t_1-(54.7°)_{\phi_2}-\tau_m-(54.7°)_{\phi_3}-\Delta-(90°)_{\phi_4}-\Delta-acq(t_2)]$ that differs by the relative phases ϕ_2 and ϕ_3 of the second and third pulses. A spectral width of 250 kHz in both dimensions, 64 t_1 values, a mixing time $\tau_m = 30$ ms, and a delay $\Delta = 20$ μs were used during the present work. The number of scans was 128. Further details, including the handling and combination of the experimental data sets, can be found elsewhere.[23,24] The sample temperature above 90 K was controlled with a Bruker BVT 1000 unit. Below 90 K, the temperature was controlled with the ITC 4 temperature control unit from Oxford Instruments. ^{13}C MAS NMR spectra were recorded at 75.47 MHz using a 4 mm Bruker MAS probe. The sample rotation frequency was 5 kHz.

Differential Scanning Calorimetry. Calorimetric studies were performed with a differential scanning calorimeter Netzsch DSC 204 (Netzsch/Selb) under nitrogen flow at heating rates of 10 °C/min.

Quantum Mechanics Calculations. Theoretical ^{2}H NMR quadrupolar coupling constants were obtained with the program package DeMon using a density functional theory approach.[25,26] To do so, an optimization of the molecular geometry was performed with the MOPAC program package (PM3 basis set).[27] DeMon simulations were done on the basis of such optimized molecular structures, employing the IGLO III basis set.

Data Processing and Simulations. The data processing of the experimental and simulated NMR signals was performed on a SUN Sparc 10 workstation using the NMRi and Sybyl software packages (Tripos, St. Louis). The theoretical simulations presented in the present work were done with appropriate FORTRAN programs, developed in our group.[28,29]

For the line shape simulations, a slow-motional approach[6,30] has been used that explicitly accounts for the interval, τ_e—responsible for spin−spin relaxation, between the $\pi/2$ pulses. The same approach then was also applicable for the analysis of the spin−spin relaxation data, as well as the partially relaxed spectra. The theoretical description of the spin−lattice relaxation data is based on the Redfield approach.[31] Here, the partially relaxed spectra were obtained after multiplication of motionally averaged ^{2}H NMR spectra (fast exchange limit) with theoretical damping factors that account for orientation-dependent spin−lattice relaxation during the interval τ_r of the inversion recovery experiment.[30] Line shape or spin−spin-relaxation effects have been neglected during this part of the data analysis. The theoretical 2D exchange ^{2}H NMR spectra were obtained following the procedures given in refs 23, 32, and 33. Exchange effects were only considered during the mixing time τ_m.

To account for the motional properties of the guest molecules, various types of dynamic models were taken into account. Thus, a two-site exchange process was found to be appropriate for the description of the trioxane ring inversion, while during the analysis of the overall rotational motions superimposed 3-site jump processes (120° jumps) and rotational diffusion processes between equally populated sites were taken into consideration. In the Appendix, further details about the theoretical approach along with some relevant publications are given.

Results and Discussion

Variable-temperature ^{2}H NMR experiments were performed on the 1,3,5-trioxane-d_6/tris-(1,2-dioxyphenyl)-cyclotriphosphazene inclusion compound between 30 and 350 K. Prior to

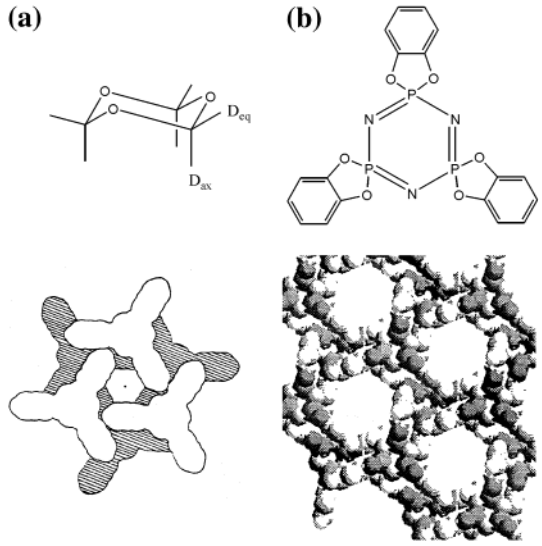

Figure 1. Chemical structures of (a) 1,3,5-trioxane and (b) tris-(1,2-dioxyphenyl)-cyclotriphosphazene and schematic drawing of the cyclophosphazene host channels (adapted from ref 11).

the NMR studies, the sample was examined by differential scanning calorimetry. From these measurements, there was no evidence for any kind of solid−solid phase transitions within the temperature range between 120 and 380 K. Attempts were made to grow single crystals for X-ray investigations, which, however, failed. From the few X-ray studies available for related cyclophosphazene inclusion compounds,[13,14] a hexagonal unit cell (space group $P6_3/m$) has been reported. This structure is consistent with the presence of hexagonal cyclophosphazene channels with an average inner diameter of 4.5 to 5.0 Å (see Figure 1), in which the guest species can be incorporated. In the following, we therefore assumed that the same structure also holds for the inclusion compound examined here. As will be shown below, the derived molecular properties of the trioxane guests strongly support this structural model for the cyclophosphazene host lattice.

In the following, we present ^{2}H NMR line shapes, spin−spin and spin−lattice relaxation, and 2D exchange experiments on the clathrate from 1,3,5-trioxane-d_6 with tris-(1,2-dioxyphenyl)-cyclotriphosphazene. Each of these experiments is known to be sensitive to a particular time-scale for molecular motion. Line shape and spin−spin relaxation experiments thus can be used to study motions in the megahertz region (10^4−10^8 s^{-1}), while spin−lattice and 2D exchange experiments are sensitive in the gigahertz (10^8−10^{11} s^{-1}) and kilohertz (10^1−10^3 s^{-1}) regions, respectively, as demonstrated during numerous studies.[3−7,33]

Figure 2 depicts a representative series of variable-temperature ^{2}H NMR spectra for the trioxane/cyclophosphazene clathrate. The typical Pake pattern, observed at $T \leq 48$ K, implies that the guest molecules are rigid on the NMR time scale, that is, $k < 10^3$ s^{-1}. It is interesting to note that the experimental splitting of 115.1 kHz between the perpendicular singularities remains unchanged down to 20 K. The derived static quadrupolar coupling constant thus is given to $e^2qQ/h = 153.5$ kHz for the deuterons in trioxane and consistent with ealier ^{2}H NMR studies.[20,34] This value, however, is considerable smaller than those reported for typical aliphatic deuterons with values in the range of 165 to 170 kHz. We therefore have performed quantum chemical calculations,[25,26] which clearly demonstrated that the smaller quadrupolar coupling constant is due to the particular chemical environment of the deuterons. Inspection of Table 1 reveals a clear tendency toward smaller quadrupolar coupling constants, if the number of oxygen atoms bound to an aliphatic carbon increases.

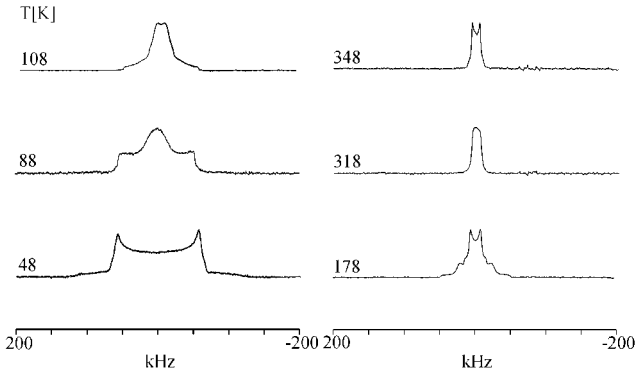

Figure 2. Variable temperature ^{2}H NMR spectra of the 1,3,5-trioxane-d_6/tris-(1,2-dioxyphenyl)-cyclotriphosphazene inclusion compound.

TABLE 1: Theoretical and Experimental ^{2}H Quadrupolar Coupling Constants

compound	$\nu_{Q,theor}$ [kHz][a]	$\nu_{Q,expt}$ [kHz]
benzene	187.7	183[b]
cyclohexane	167.8	166.7[c]
1,4-dioxane	163.4	
trioxane	157.9	153.5[d]
		152[e]
		153.3[f]

[a] Calculated with the quantum-chemical program deMon (see Experimental Section). [b] Ok, J. H.; Vold, R. R.; Etter, M. C. *J. Phys. Chem.* **1989**, *93*, 7618. [c] Poupko, R.; Furman, E.; Müller, K.; Luz, Z. *J. Phys. Chem.* **1991**, *95*, 407. [d] This work. [e] Gelerinter, E.; Luz, Z.; Poupko, R.; Zimmermann, H. *J. Phys. Chem.* **1990**, *94*, 8845. [f] Gelerinter, E.; Luz, Z.; Poupko, R.; Zimmermann, H. *J. Phys. Chem.* **1990**, *94*, 5391.

At temperatures $T > 48$ K, characteristic spectral changes are registered that imply the onset of guest motions that enter the sensitive range of ^{2}H NMR line shapes. A closer inspection of Figure 2 reveals that at 178 K the ^{2}H NMR spectrum consists of two axially symmetric subspectra of reduced spectral widths and a ratio of the experimental splittings of about 3:1. Upon further heating above room temperature, eventually a single, axially symmetric ^{2}H NMR spectrum remains, as shown exemplary in the spectrum recorded at 348 K. In the following, we will discuss separately the low-temperature range up to 200 K and the high-temperature range between 200 and 350 K. It should be kept in mind that this subdivision is solely based on the observed spectral effects, because from the calorimetric studies there was no evidence for a solid−solid transition between 120 and 370 K.

A. Dynamics in the Low-Temperature Range. Figure 3 depicts experimental ^{2}H NMR spectra covering the low-temperature range along with their best simulations, as given in the center column. To understand the experimental ^{2}H NMR line shape effects, various types of motional models for the trioxane dynamics have been examined. In fact, two motional contributions were found to be necessary to describe the experimental line shape effects: (i) rotation of the trioxane molecules around their C_3-symmetry axes; (ii) rotational motion around the host channel long axis. As a consequence of the former rotation around the molecular C_3-axis, ^{2}H NMR spectra in the low-temperature range up to 200 K can be regarded as a superposition of two subspectra that refer to the axial and equatorial deuterons. In the *fast exchange limit*, the splittings between the perpendicular singularities of the individual sub-

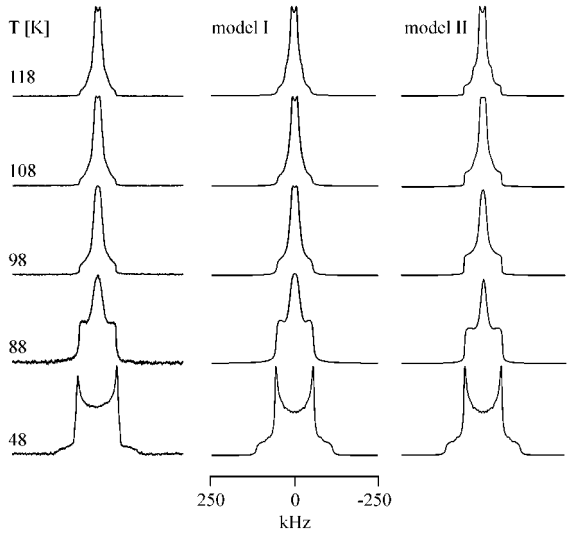

Figure 3. Experimental (left column) and theoretical ^{2}H NMR spectra of 1,3,5-trioxane-d_6 in tris-(1,2-dioxyphenyl)-cyclotriphosphazene. The theoretical ^{2}H NMR spectra were obtained by using motional model I (center column) and motional model II (right column). The correlation times for the simulations with model I can be taken from the Arrhenius plots in Figure 8. For the simulations with model II, the following correlation times have been used: at 48 K, $\tau_{C_3} = \tau_{CH} > 10^{-3}$ s; at 88 K, $\tau_{C_3} = 7 \times 10^{-7}$ s, $\tau_{CH} = 6 \times 10^{-7}$ s; at 98 K, $\tau_{C_3} = 1.5 \times 10^{-7}$ s, $\tau_{CH} = 2 \times 10^{-7}$ s; at 108 K, $\tau_{C_3} = 6 \times 10^{-8}$ s, $\tau_{CH} = 7 \times 10^{-8}$ s; at 118 K, $\tau_{C_3} = 2 \times 10^{-8}$ s, $\tau_{CH} = 3 \times 10^{-8}$ s. τ_{C_3} denotes the correlation time for rotation around the molecular C_3-axis; τ_{CH} denotes the correlation time for rotation around the channel axis.

spectra are therefore given by[4]

$$\langle \Delta\nu \rangle_i = \frac{3}{4}\nu_{Q,stat}\frac{1}{2}(3\cos^2\Theta_{1,i} - 1); \quad i = \text{ax, eq} \qquad (1)$$

In this expression, $\nu_{Q,stat} = e^2qQ/h$ is the quadrupolar coupling constant, and Θ_1 is the angle between the C$-^2$H bond and the molecular C_3-axis. From semiempirical quantum chemical calculations (see Experimental Section[27]), the angles between the C$-^2$H bond and the C_3-axis were found to 0° and 108.3° for the axial and equatorial deuterons, respectively. Inserting these values into eq 1 yields a ratio for the splittings of the subspectra $\langle \Delta\nu \rangle_{ax}/\langle \Delta\nu \rangle_{eq}$ = 1:0.35 in agreement with the experimental findings (see Figure 1).

The comparison of the absolute splittings revealed that the theoretical value is much higher than the experimental one. This discrepancy can be explained by the presence of two additional fast motional contributions, namely, the aforementioned second rotational motion around the channel axis and fast molecular fluctuations. The above expression thus has to be extended by a factor of $^1/_2(3\cos^2\Theta_2 - 1)$ that accounts for rotation about the channel long axis. In addition, ν_Q has to be replaced by the scaled value $\langle \nu_Q \rangle$ because of the high-frequency (overall molecular) fluctuations (see below). The final expression in the *fast motional limit* is then given by

$$\langle \Delta\nu \rangle_i = \frac{3}{4}\langle \nu_Q \rangle\frac{1}{2}(3\cos^2\Theta_{1,i} - 1)\frac{1}{2}(3\cos^2\Theta_2 - 1); \quad i = \text{ax, eq} \qquad (2)$$

Here, the angle Θ_2 refers to the orientation of the C_3-axis of the trioxane molecules with respect to the channel long axis.

The presence of a second rotational motion unequivocally could be proven by the observed ^{2}H NMR line shape effects in the *intermediate motional range* below 100 K. Here, extensive model simulations have been performed to describe the observed

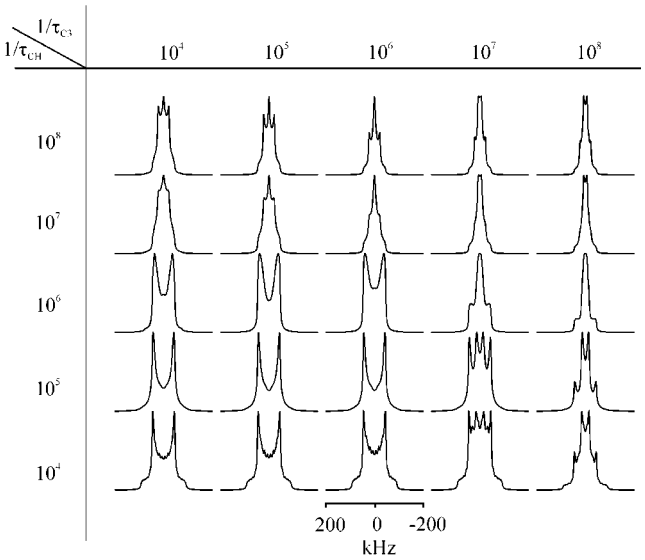

Figure 4. Theoretical ^{2}H NMR line shapes for 1,3,5-trioxane-d_6 obtained with model I by varying the correlation times of both rotational motions. $1/\tau_i$ is given in s^{-1}. $\theta_2 = 90°$.

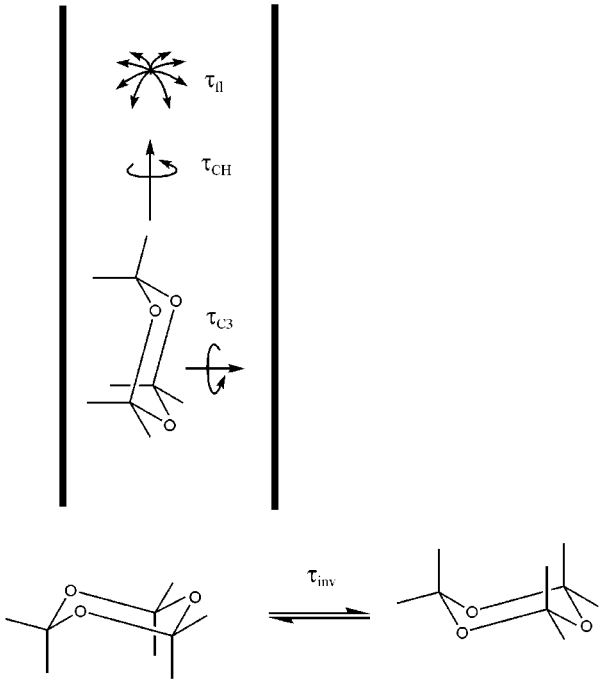

Figure 5. Schematic drawing of the proposed trioxane motions in the inclusion compound with tris-(1,2-dioxyphenyl)-cyclotriphosphazene.

^{2}H line shape changes between about 50 and 100 K. These theoretical calculations clearly demonstrated that two superimposed rotational motions must be present. A representative series of theoretical spectra is given in Figure 4, which reveals a significant influence by both types of overall rotational motion. The line shape simulations have further shown that the symmetry axes of both rotations set up an angle of 90° ± 2°; the molecular C_3-symmetry axes of the trioxane molecules are thus oriented perpendicular with respect to the cyclophosphazene channel long axis, as shown schematically in Figure 5.

The derived absolute orientation of the trioxane guests is a direct consequence of the spatial constraints imposed by the cyclophosphazene lattice, as can be deduced from an inspection of the molecular dimensions of the trioxane guests and the cyclophosphazene host channel diameter. This is in agreement with a former ^{2}H NMR study on the benzene/cyclophosphazene

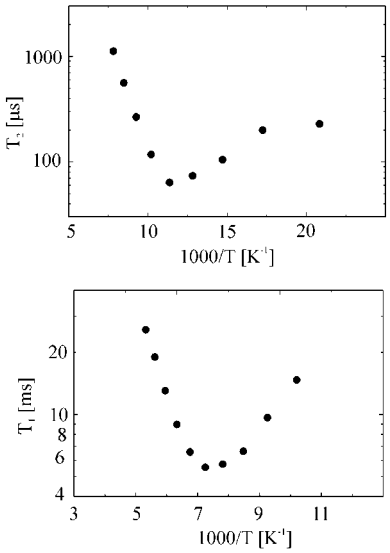

Figure 6. Experimental ^{2}H spin−spin (top) and spin−lattice (bottom) relaxation times of 1,3,5-trioxane-d_6 in tris-(1,2-dioxyphenyl)-cyclotriphosphazene.

inclusion compound,[15,16] in which the molecular C_6-axes of the benzene guests also were found to be oriented perpendicular with respect to the host channel long axis.

In addition, the model simulations have demonstrated that the best reproduction of the experimental spectra could be achieved by a 3-fold jump motion (120° jumps between equally populated sites) for the rotation around the channel axis and a diffusive process for rotation around the molecular C_3-symmetry axis (model I). This is shown in Figure 3, in which the experimental ^{2}H NMR spectra are contrasted with the best fit spectra from the simulations with this favored motional model (center column). For comparison, in the right column, the best fit spectra are given for model II, in which both rotational motions were described by 3-fold jumps. In particular, the experimental ^{2}H NMR spectra at 88 and 98 K are better reproduced by the mixed jump/diffusive model (model I) than by model II (jump/jump model). It should be mentioned that we have also examined the possibilities of (i) diffusive motions for both the channel axis and C_3-axis rotation (model III) and (ii) diffusive motion for channel axis rotation and 3-fold jump process for C_3-axis rotation (model IV), which, however, are less likely due to the interior cyclophosphazene channel structure (see below). For both of these models, even larger deviations between the theoretical and experimental spectra have been found.

The quality of motional model I has been further examined by the analysis of the partially relaxed spectra from the quadrupole echo experiment.[35] The experimental spin−spin relaxation data, given in Figure 6, exhibit a typical T_2-minimum at 88 K, which marks the temperature at which the rate constant of some molecular motion matches the size of the quadrupolar interaction. In Figure 7, partially relaxed spectra are given that refer to the T_2-minimum at 88 K. Again, the experimental spectra are well reproduced by their theoretical counterparts based on model I. For comparison, the best fit spectra for model II are also shown. As before, model I provides a better reproduction of the experimental ^{2}H NMR spectra than model II. Theoretical spectra also have been calculated on the basis of the other motional models (models III and IV), mentioned above. In none of these cases, a similar good fit could be achieved as provided by model I, which is a further support for our model assumption. In quite the same way, we have analyzed

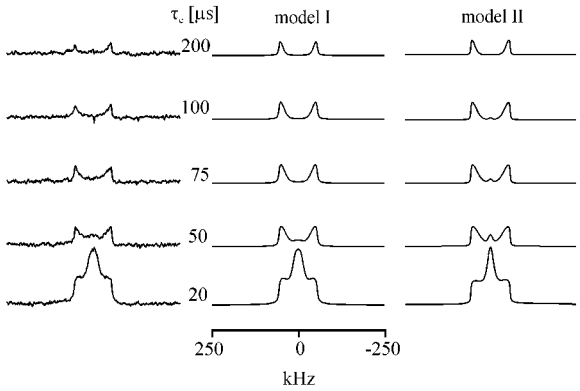

Figure 7. Experimental (left column), recorded at 88 K, and theoretical partially relaxed ^{2}H NMR spectra of 1,3,5-trioxane-d_6 in tris-(1,2-dioxyphenyl)-cyclotriphosphazene obtained via the quadrupole echo sequence. The theoretical spectra were calculated on the basis of model I (center column; for correlation times, see Figure 8) and with model II (right column; $\tau_{C_3} = 7 \times 10^{-7}$ s, $\tau_{CH} = 6 \times 10^{-7}$ s).

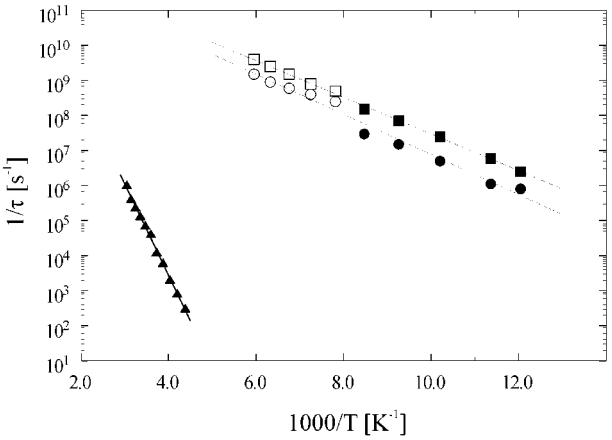

Figure 8. Arrhenius plot for the overall rotational motions and ring inversion process of 1,3,5-trioxane-d_6 in tris-(1,2-dioxyphenyl)-cyclotriphosphazene: (○, ●) τ_{CH}, rotation around channel axis; (□, ■) τ_{C_3}, rotation around C_3-axis (open symbols represent data from analyis of partially relaxed spectra from inversion recovery experiments; full symbols represent data from partially relaxed spectra from quadrupole echo experiments and line shape studies); (▲) τ_{inv}, ring inversion (from line shape analysis).

the partially relaxed ^{2}H NMR spectra (quadrupole echo experiment) at other temperatures around the T_2-minimum. The derived correlation times for both overall rotational motions, obtained from the line shape simulations, as well as the partially relaxed quadrupolar echo spectra, are summarized in the Arrhenius plots in Figure 8. Here, for the jump model with equally populated sites, the correlation time τ_{CH} (CH denotes rotation around the channel axis) is related to the first-order rate constant k by (P = relative population of the sites)

$$\frac{1}{\tau_{CH}} = \frac{k}{P} \tag{3}$$

For the diffusive motion, the following expression for the correlation times τ_{C_3} (C_3 denotes rotation around the molecular C_3-axis) holds:

$$\frac{1}{\tau_{C_3}} = \left(\frac{2\pi}{N}\right)^2 6k \tag{4}$$

Here, N is the number of orientations, and k is the first-order rate constant for the transition between neighboring sites.[6]

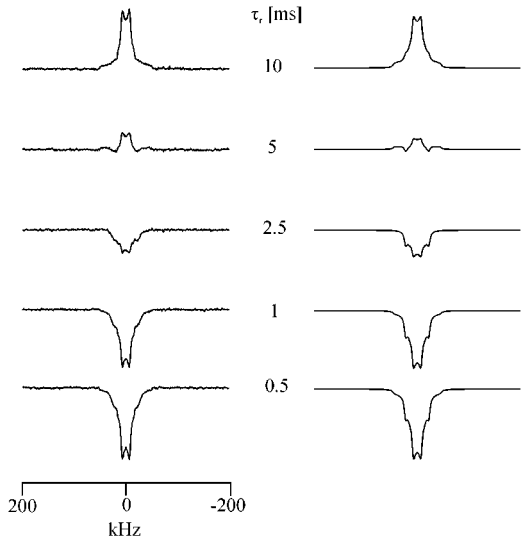

Figure 9. Experimental (left column), recorded at 148 K, and theoretical (right column) partially relaxed ^{2}H NMR spectra of 1,3,5-trioxane-d_6 in tris-(1,2-dioxyphenyl)-cyclotriphosphazene obtained via the inversion recovery sequence. The theoretical spectra were calculated on the basis of model I and the correlation times given in Figure 8.

At temperatures above 118 K, the molecular motions are too fast and cannot affect the ^{2}H NMR line shapes and the spin−spin relaxation data. Here, we have analyzed the spin−lattice relaxation times (see Figure 6), as well as partially relaxed spectra from the inversion recovery experiment.[30] Again, the T_1-curve exhibits a pronounced minimum at 140 K, which originates from the same overall rotational motions discussed above. Figure 9 depicts experimental partially relaxed ^{2}H NMR spectra from the inversion recovery experiment. The theoretical spectra, shown in the same figure, were obtained on the basis of model I. As before, an excellent reproduction of the experimental spectra could be achieved, which strongly supports the validity for our motional model. The correlation times derived from the analysis of these partially relaxed spectra (inversion recovery experiment) in the vicinity of the T_1-minimum are given in Figure 8 (open symbols). It can be seen that the data derived from the analysis of the quadrupole echo and the inversion recovery experiments fit nicely, yielding an almost straight line in the Arrhenius plot.

Inspection of Figure 8 reveals that, although both rotational motions are decoupled from each other, accidentally they are on a very similar time scale. From the slope of both curves, activation energies of 10.0 and 10.9 kJ/mol for the rotation around the C_3-symmetry axis and channel long axis, respectively, have been derived (see Table 2). Such small activation energies for overall rotational motions at first sight are somewhat surprising. However, in the aforementioned study of the benzene/cyclophosphazene inclusion compound,[15] a 3-fold jump rotation of the guests around the channel long axis also has been reported along with a relatively low activation energy of 16.7 kJ/mol. The observation of a 3-fold jump rotation can be attributed to the fact that the interior cyclophosphazene channel structure forms distinct lobes.[15,17] As a result, the potential energy curve against rotation of the guest molecules around the cyclophosphazene channel long axis exhibits pronounced minima, separated by 120°, that refer to the three jump sites. The energy barrier between adjacent sites must be rather low, as can be deduced from the low activation energies derived for this rotational process.

Rotational motions around the C_3-axis of the trioxane guests can be compared with data published for the cyclohexane/thiourea[36] and trioxane/urea[20] inclusion compounds with values of 10.5 and 20.0 kJ/mol, respectively. Again, for these inclusion compounds, the rotational motions around the C_3-axis of six-membered-ring guests are relatively unhindered. On the contrary, for pure trioxane,[34] a much higher activation energy of 79.5 kJ/mol and considerably lower absolute values for the rate constants of the C_3-rotational motion (more than 3 orders of magnitude) have been reported, which certainly are a direct consequence of the close crystal packing in pure trioxane. It is worthwhile to note that in these systems the C_3-axis rotation was ascribed to a 3-fold jump process, while in the present study, as outlined above, a diffusive process was found to be more appropriate. This points to a unique property of the trioxane/cyclophosphazene inclusion compound with only a small variation of the potential energy with rotation about the molecular C_3-axis of the trioxane guests, along with a minor sterical hindrance by the host lattice. It should be noted that preliminary data are available for the cyclohexane/cyclophosphazene inclusion compound.[37] Unlike the situation for the trioxane guests, the cyclohexane molecules are found to undergo 120° jumps around their C_3-symmetry axes. The corresponding potential energy curve thus should exhibit well-pronounced minima, most probably due to a larger sterical hindrance from the additional CH_2-groups in the cyclohexane molecules. In summary, the small activation energies, derived for both overall rotational motions in the trioxane/cyclophosphazene inclusion compound, strongly suggest that the interactions between the host channels and the guest species are rather weak. As mentioned earlier, for the simulations in Figures 3, 7, and 9, apart from the two rotational motions, additional overall molecular fluctuations had to be taken into account. They, however, were too fast and therefore did not directly contribute to spin relaxation. Rather, they give rise to a reduction of the quadrupolar splitting, as will be discussed below. In summary, the present analysis of the low-temperature ^{2}H NMR data is based on relatively simple models for overall reorientational motions that nevertheless provided a good reproduction of the experimental data. It might well be that other models—such as rotational oscillations, which so far have not been examined—are also appropriate for the description of the present guest−host system. Here, 2D exchange NMR experiments would be of great help,[38] which for technical reasons could not be performed in the low-temperature range.

TABLE 2: Kinetic Parameters for Various Guest Motions in Inclusion Compounds

compound	preexponential factor [s^{-1}]	activation energy [kJ/mol]
A. Rotation around Channel Axis		
trioxane/cyclophosphazene[a]	4×10^{12}	10.9
C_6D_6/cyclophosphazene[b]		16.7
B. Rotation around Molecular C_3-Axis		
trioxane/cyclophosphazene[a]	5.1×10^{12}	10.0
trioxane/urea[c]	2.2×10^{13}	20.0
trioxane (pure)[d]	2.3×10^{18}	79.5
cyclohexane/thiourea[e]	1.8×10^{13}	10.5
C. Ring Inversion		
trioxane/cyclophosphazene[a]	7.5×10^{13}	50.0
trioxane/urea[c]	2.7×10^{13}	48.9
trioxane/liquid crystalline solution[d]	1.5×10^{14}	51.0
cyclohexane/thiourea[e]	1.1×10^{13}	46.4

[a] This work. [b] Meirovitch, E.; Belsky, I.; Vega, S. *J. Phys. Chem.* **1984**, *88*, 1522. [c] Gelerinter, E.; Luz, Z.; Poupko, R.; Zimmermann, H. *J. Phys. Chem.* **1990**, *94*, 5391. [d] Gelerinter, E.; Luz, Z.; Poupko, R.; Zimmermann, H. *J. Phys. Chem.* **1990**, *94*, 8845. [e] Poupko, R.; Furman, E.; Müller, K.; Luz, Z. *J. Phys. Chem.* **1991**, *95*, 407.

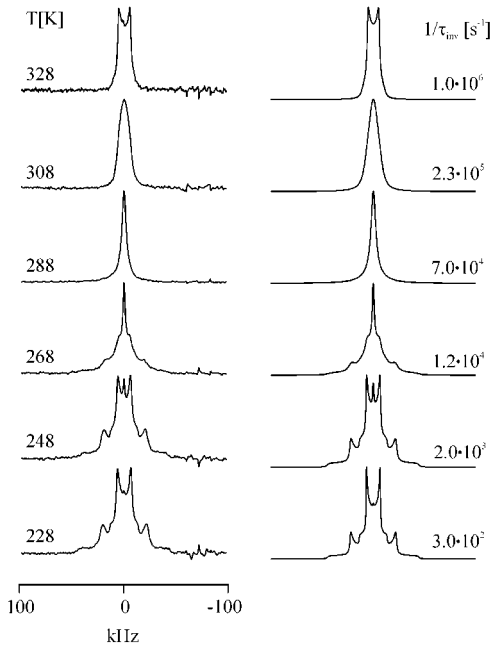

Figure 10. Experimental (left column) and theoretical (right column) ^{2}H NMR spectra of 1,3,5-trioxane-d_6 in tris-(1,2-dioxyphenyl)-cyclotriphosphazene. The theoretical ^{2}H NMR spectra were obtained on the basis of a ring inversion process of the trioxane guests, modeled with a two-site exchange process.

B. Dynamics in the High-Temperature Range. Representative ^{2}H NMR spectra for the high-temperature range between 200 and 370 K are given in Figure 10. Again, characteristic spectral changes are observed, which, as found previously for the trioxane/urea inclusion compound,[20] can be attributed to the ring inversion process of the trioxane guests. This process can be described by a mutual (two-site) exchange process of the axial and equatorial deuterons. As a result, at elevated temperatures, as soon as the rate constant of the ring inversion process approaches the size of the quadrupolar coupling constant, the subspectra due to both types of deuterons merge. In the *fast exchange* spectrum at 328 K, thus again a typical Pake pattern is visible, which is the weighted average of the subspectra from the axial and equatorial deuterons. Here, the experimental splitting should be given by

$$\langle \Delta\nu \rangle_{ave} = \frac{1}{2}[\langle \Delta\nu \rangle_{ax} - \langle \Delta\nu \rangle_{eq}] \qquad (5)$$

In this equation, $\langle \Delta\nu \rangle_{ax}$ and $\langle \Delta\nu \rangle_{eq}$ refer to the experimental splittings of the subspectra due to the axial and equatorial deuterons at $T = 228$ K, that is, the slow motional limit for the ring inversion process. The minus sign reflects the fact that the motional averaging due to overall rotation (see eqs 1 and 2) yields opposite signs for $\langle \Delta\nu \rangle_i$ of the axial and equatorial deuterons. It is observed that the experimental value of $\langle \Delta\nu \rangle_{ave}$ in the fast exchange limit is somewhat smaller than the expected one from eq 5. This again can be attributed to an orientational disorder due to the above-mentioned fast molecular fluctuations the amplitudes of which increase with temperature.

A further independent proof for the presence of the intramolecular ring inversions can be provided by 2D exchange NMR experiments.[23,33] In Figure 11, a 2D exchange ^{2}H NMR spectrum is given that has been recorded at 220 K, at which the ring inversion process is in the slow exchange limit. Again, the characteristic exchange pattern in the experimental spectrum can be reproduced by the theoretical counterpart, which was obtained on the basis of an underlying ring inversion (modeled by a 2-site jump process). In principle, such 2D exchange NMR experiments could be further used to extend the accessible dynamic range toward smaller rate constants.[33] In the present case, we have refrained from doing so, because the line shape analysis provided sufficient experimental data points for the ring inversion dynamics.

The derived rate constants for this internal process are also plotted in Figure 8. It is quite obvious that the ring inversion is characterized by a much higher activation energy (50.0 kJ/mol) than that found for the above-mentioned overall rotational motions. However, such high activation energies for ring inversion of six-membered-ring systems are very common. In fact, it turns out that the activation energy is very close to the value reported from the studies on the trioxane/urea inclusion compound[20] and a liquid crystalline solution with trioxane[34] (see Table 2). In this respect, the present cyclophosphazene systems resemble other thiourea and urea inclusion compounds with six-membered-ring guests.[36,39] Obviously, the time scale and activation energies of such intramolecular guest motions are almost unaffected by the particular host lattice.

C. Molecular Ordering. Besides the motional properties of the trioxane guests, also structural information could be obtained. As outlined above, the C_3-axes of the guest molecules are oriented perpendicular with respect to the channel long axis. At elevated temperatures, such a fixed orientation, however, is lost due to the presence of fast overall molecular fluctuations in an axially symmetric ordering potential. They give rise to an increase of orientational disorder, as reflected by the reduction of the experimental spectral widths. The degree of orientational disorder of the guest species, solely arising from molecular fluctuations, can be expressed in terms of an orientational order parameter S_{mol}[20,36] defined as

$$\langle n_Q \rangle = \nu_{Q,stat} S_{mol} \qquad (6)$$

The value of $\langle \nu_Q \rangle$, the experimental quadrupolar coupling constant, either is taken directly from the NMR spectra (in the slow exchange or fast exchange limit) or from the input parameters of the corresponding line shape simulations. On this basis, S_{mol} was determined for the whole temperature range between 40 and 350 K. Inspection of the data in Figure 12 reveals a continuous decrease of orientational order with temperature, which can be understood by an increase of the fluctuation amplitude in the same direction. At 350 K, a lower limit of $S_{mol} \approx 0.6$ is reached, being considerable higher than that of $S_{mol} \approx 0.1$, reported for the trioxane/urea[20] and cyclohexane/thiourea[36] inclusion compounds. This higher orientational order can be traced back to the larger spatial constraints in the cyclophosphazene guest−host system, most probably due to the smaller diameter of the cyclophosphazene channels. Whether the observed increase of orientational disorder also reflects a temperature-dependent widening of the cyclophosphazene channels is unknown, because variable-temperature X-ray data of these compounds so far have not been reported.

In this context, the question might arise whether at low temperatures, at which the rotational motions are frozen in, a preferential orientation of the trioxane guests exists in the horizontal direction. The present data on polycrystalline samples cannot answer this question; here, single-crystal studies are required. It might well be that at temperatures below 30 K an additional solid−solid phase transition along with a distortion of the hexagonal host channel occurs, which imposes a distinct

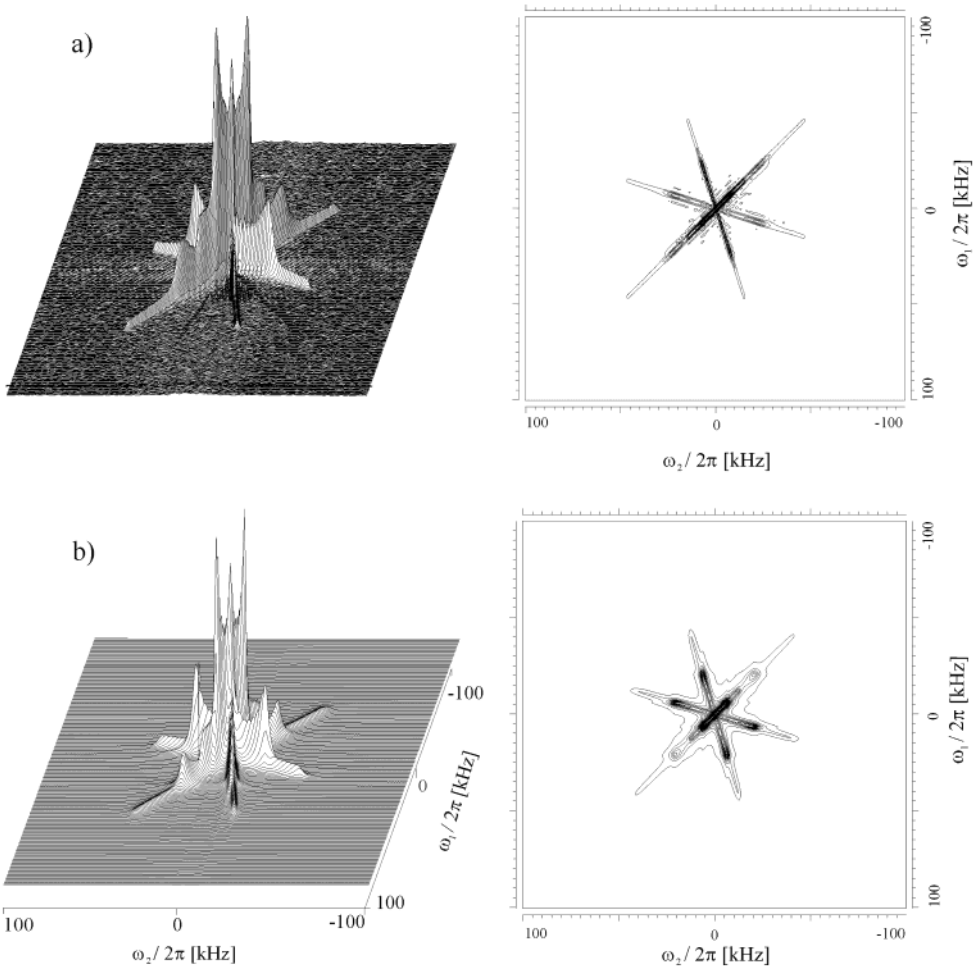

Figure 11. Experimental (a) and theoretical (b) ^{2}H 2D exchange NMR spectrum of 1,3,5-trioxane-d_6 in tris-(1,2-dioxyphenyl)-cyclotriphosphazene recorded at 208 K. The mixing time, τ_m, was 20 ms. The theoretical ^{2}H NMR spectrum was calculated on the basis of a ring inversion process of the trioxane guests and with the condition of $(1/\tau_{inv})\tau_m \gg 1$ (τ_{inv} denotes the correlation time for ring inversion).

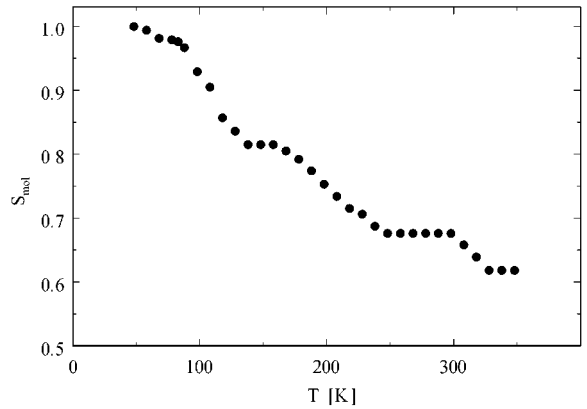

Figure 12. The molecular order parameter of the trioxane guests as function of temperature in the inclusion compound with tris-(1,2-dioxyphenyl)-cyclotriphosphazene.

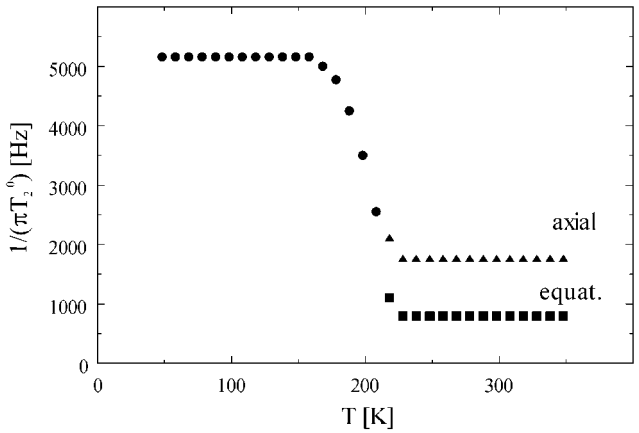

Figure 13. Residual line widths, $1/(\pi T_2^0)$, derived for the axial and equatorial deuterons in trioxane as function of temperature for the inclusion compound with tris-(1,2-dioxyphenyl)-cyclotriphosphazene.

horizontal alignment (perpendicular to the channel axis) of the trioxane guests. Similar observations have been reported earlier, for example, for *n*-alkane/urea inclusion compounds.[40]

In Figure 13, the residual line widths, $1/(\pi T_2^0)$, which were used as input parameters during the line shape simulations, are plotted as a function of temperature. It can be seen that at temperatures below 150 K the residual line widths are almost temperature-independent with the same values for both the axial and equatorial deuterons. At about 170 K, the residual line widths drop down considerably to values of 1750 and 800 Hz for the axial and equatorial deuterons, respectively. Above this temperature, again temperature-independent line widths are registered. In the present case, the experimental line widths are dominated by two contributions: (i) intramolecular dipolar interactions between the deuterons of the methylene groups and (ii) intermolecular dipolar interactions between the deuterons of the trioxane molecules and the protons from cyclophosphazene. As for other magnetic interactions, changes of the residual line widths can mark the onset of molecular motions that affect the underlying dipolar couplings.

In the present case, rotational and fluctuational motions, as well as ring inversions, can be ruled out to be responsible for the experimental line width effects, because these motions show up in quite different temperature regions. The only remaining motional processes are therefore lateral displacements of the trioxane guests that also might reduce the intermolecular deuteron−proton dipolar couplings. However, a final proof for this assumption is not possible on the basis of our present ^{2}H NMR data. Another explanation of the line width reduction can be given by structural changes in the host channel region, comprising rearrangements of the phenylene groups or widening of the channel diameter or both. In this connection, it is interesting to note that at higher temperatures the axial deuterons possess a higher line width than the equatorial ones. This again is in line with the general picture that the C_3-axes of the trioxane molecules are oriented perpendicular the channel long axis, because here the average distance between the axial deuterons and the host matrix would be somewhat shorter than that for the equatorial deuterons. Forthcoming studies, comprising double resonance experiments, might provide further information on this topic.

Conclusions

The molecular behavior of perdeuterated 1,3,5-trioxane-d_6 in a cyclophosphazene inclusion compound has been studied by dynamic ^{2}H NMR spectroscopy. The analysis of the experimental data revealed a relatively complex motional behavior of the trioxane guests in the cyclophosphazene host channels. The guest molecules thus undergo rotational motions (diffusive process) around their C_3-axes, as well as rotations around the channel long axis (3-fold jumps), which dominate the relaxation data below 120 K. The molecular C_3-axes were found to be oriented perpendicular with respect to the channel long axis. These findings clearly prove that the orientation of the trioxane guests and their rotational motions directly reflect the overall (interior) shape of the cylophosphazene channels. The ring inversion process, which dominates the NMR line shapes above 200 K, is almost unaffected by the host lattice. Thus, activation parameters were derived that are almost identical with those reported from solution NMR studies. The present NMR study has further shown that high-frequency fluctuations of the guest molecules exist that give rise to a substantial orientational disorder at higher temperatures. The orientational order of the trioxane guests, however, is considerably higher than that reported for other inclusion compounds with six-membered-ring guests, most probably because of the larger spatial constraints by the smaller cyclophosphazene channels. At present, other cyclophosphazene inclusion compounds with six-membered-ring systems are being studied to evaluate the impact of the actual guest structure on the behavior of the guest molecules.

Acknowledgment. We thank Mrs. D. Zauser and Mrs. H. Seidel for the synthesis of the compounds used in the present study. We are indebted to Prof. U. Haeberlen (MPI für Medizinische Forschung, Heidelberg) for his support during the low-temperature measurements. The authors are also grateful to Prof. M. Kaupp (Universität Würzburg) for the support during the quantum chemical calculations. Financial support by the Deutsche Forschungsgemeinschaft and the Fonds der Chemischen Industrie is gratefully acknowledged.

Appendix

In the following, we briefly review the theoretical background for the simulations of dynamic ^{2}H NMR experiments. As outlined elsewhere,[4−7,30,35] the free induction decay starting at the top of the quadrupole echo is given by

$$S(t,2\tau_e) = \mathbf{1}\cdot\exp(\mathbf{A}t)\cdot\exp(\mathbf{A}\tau_e)\cdot\exp(\mathbf{A}\tau_e)^*\cdot\mathbf{P}(0) \quad \text{(A1)}$$

The vector $\mathbf{P}(0)$ contains the fractional populations of the N exchanging sites in thermal equilibrium. The term $\mathbf{A}$ is a complex matrix of size N with

$$\mathbf{A} = i\cdot\mathbf{\Omega} + \mathbf{K} \quad \text{(A2)}$$

The imaginary part of $\mathbf{A}$ is given by the diagonal matrix $\mathbf{\Omega}$ of which the elements, ω_{ii}, describe the frequencies of the exchanging sites. The real part corresponds to a kinetic matrix, $\mathbf{K}$. Here, the nondiagonal elements, k_{ij}, are the jump rates from site j to i, while the diagonal elements k_{ii} represent the sums of the jump rates for leaving site i and contain the residual line widths in terms of $1/T_2^0$. Depending on the complexity of the system studied, several internal and intermolecular processes can be superimposed. For the present case, the biggest matrix has a size of $N = 60$ due to three sites for the 3-fold jumps around the channel axis and 20 sites for rotation around the C_3-axis (model I, jump/diffusion model). For the ring inversion process, a program version was employed accounting for only two interchanging sites. Equation A1 is solved numerically using standard diagonalization routines, from which ^{2}H NMR line shapes, partially relaxed spectra, and spin−spin relaxation times are derived.

The simulation of partially relaxed ^{2}H NMR spectra from the modified inversion recovery experiment (see Experimental Section) is feasible with the help of eq A3,[30]

$$S(t,2\tau_e,\tau_r) = [1 - 2\exp(-\tau_r/T_1)]S(t,2\tau_e) \quad \text{(A3)}$$

τ_r refers to the relaxation interval between the inversion pulse and the quadrupole echo sequence used for signal detection. The spin−lattice relaxation time, T_1, is obtained from

$$\frac{1}{T_1} = \frac{3}{16}\left(\frac{e^2qQ}{\hbar}\right)^2 [J_1(\omega) + 4J_2(2\omega)] \quad \text{(A4)}$$

The spectral densities, J_m, can be derived by solving the following equation for a general N-site exchange:[41,42]

$$J_m(\omega) = 2\sum_{a,a'=-2}^{2} d^{(2)}_{ma}(\theta')d^{(2)}_{ma'}(\theta')\sum_{n,l,j=1}^{N} X_l^{(0)}X_l^{(n)}X_j^{(0)}X_j^{(n)}d^{(2)}_{0a}(\theta_l'')d^{(2)}_{0a}(\theta_j'')\cos(a\phi_l - a'\phi_j)\frac{\lambda_n}{\lambda_n^2 + \omega^2}$$
$$\text{with} \quad \phi_i = \phi_i'' - \phi' \quad \text{(A5)}$$

Here, $X^{(n)}$ and λ_n are the corresponding eigenvectors and eigenvalues of the symmetrized rate matrix, $\mathbf{K}'$, the angles θ'' and ϕ'' are the polar angles between the principal axis and an intermediate axis (motional axis) system, and the angles θ' and ϕ' are those between the intermediate and the laboratory axis system, respectively. The $d^{(2)}_{ab}(\theta)$ parameters are elements of the reduced Wigner rotation matrix. If there is a superposition of several motional modes, then the transformation from the principal axis system to the laboratory frame is subdivided into several steps according to the number of motional contributions.

For the theoretical description of the 2D exchange experiments, the quadrupolar order (S_Q) and Zeeman order (S_Z) signals

are calculated according to the following equations[23,32,33]

$$S_Q(t_1,t_2;\tau_m) = C\sum_{ij}\sin(\omega_Q{}^i t_1)\exp(-t_1/T_2{}^i)\,P_{ij}(\tau_m)\times \sin(\omega_Q{}^j t_2)\exp(-t_2/T_2{}^j)$$

$$S_Z(t_1,t_2;\tau_m) = C\sum_{ij}\cos(\omega_Q{}^i t_1)\exp(-t_1/T_2{}^i)\,P_{ij}(\tau_m)\times \cos(\omega_Q{}^j t_2)\exp(-t_2/T_2{}^j)$$

$$\text{with}\quad P_{ij}(\tau_m) = P_i[\exp(\mathbf{K}\cdot\tau_m)]_{ij} \qquad \text{(A6)}$$

P_{ij} and P_i denote the conditional probability that a nucleus jumps from site j to site i during τ_m and the equilibrium population of site i, respectively. **K** is the exchange matrix, already introduced above. In equation A6, spin−lattice relaxation contributions during τ_m have been neglected. The processing of both data sets is described elsewhere.[23,24]

References and Notes

(1) Atwood, J. L., Davies, J. E. D., MacNicol, D. D., Eds. *Inclusion Compounds*; Academic Press: New York, 1984; Vols. 1−3; Oxford University Press: Oxford, 1991; Vols. 4 and 5.

(2) Atwood, J. L., Davies, J. E. D., MacNicol, D. D., Voegtle, E., Eds. *Comprehensive Supramolecular Chemistry*; Pergamon Press: London, 1996.

(3) Ripmeester, J. In *Inclusion Compounds*; Atwood, J. L., Davies, J. E. D., MacNicol, D. D., Eds.; Oxford University Press: 1991; Vol. 5, p 37.

(4) Griffin, R. G. *Methods Enzymol*. **1981**, *72*, 108.

(5) Spiess, H. W. *Adv. Polym. Sci*. **1985**, *66*, 23.

(6) Müller, K.; Meier, P.; Kothe, G. *Prog. Nucl. Magn. Reson. Spectrosc*. **1985**, *17*, 211.

(7) Vold, R. R.; Vold, R. L. *Adv. Magn. Opt. Res*. **1991**, *16*, 85.

(8) Schlenk, W. *Liebigs Ann. Chem*. **1949**, *204*, 565; **1951**, *573*, 142.

(9) Hollingsworth, M. D.; Harris, K. D. M. In *Comprehensive Supramolecular Chemistry*; Atwood, J. L., Davies, J. E. D., MacNicol, D. D., Voegtle, E., Eds.; Pergamon Press: London, 1996; Vol. 6, p 177.

(10) Allcock, H. R. In *Inclusion Compounds*; Atwood, L. J., Davies, J. E. D., MacNicol, D. D., Eds.; Academic Press: New York, 1984; Vol. 1, p 351.

(11) Allcock, H. R. *Acc. Chem. Res*. **1978**, *11*, 81.

(12) Allcock, H. R. *J. Am. Chem. Soc*. **1964**, *86*, 2591.

(13) Allcock, H. R.; Stein, M. T. *J. Am. Chem. Soc*. **1974**, *96*, 49.

(14) Allcock, H. R.; Allen, R. W.; Bissell, E. C.; Smeltz, L. A.; Teeter, M. *J. Am. Chem. Soc*. **1976**, *98*, 5120.

(15) Meirovitch, E.; Belsky, I.; Vega, S. *J. Phys. Chem*. **1984**, *88*, 1522.

(16) Meirovitch, E.; Belsky, I. *J. Phys. Chem*. **1984**, *88*, 4308.

(17) Meirovitch, E.; Rananavare, S. B.; Freed, J. H. *J. Phys. Chem*. **1987**, *91*, 5014.

(18) Meirovitch, E. *J. Phys. Chem*. **1984**, *88*, 6411.

(19) Liebelt, A.; Müller, K. *Mol. Cryst. Liq. Cryst*. **1998**, *313*, l45.

(20) Gelerinter, E.; Luz, Z.; Poupko, R.; Zimmermann, H. *J. Phys. Chem*. **1990**, *94*, 5391.

(21) Allcock, H. R.; Kugel, R. L. *Inorg. Chem*. **1966**, *5*, 1016.

(22) Heaton, N. J.; Vold, R. R.; Vold, R. L. *J. Magn. Reson*. **1988**, *77*, 572.

(23) Schmidt, C.; Blümich, B.; Spiess, H. W. *J. Magn. Reson*. **1988**, *79*, 269.

(24) Blümich, B.; Spiess, H. W. *Angew. Chem*. **1988**, *100*, 1716.

(25) Malkin, V. G.; Malkina, O. L.; Casida, M. E.; Salahub, D. R. *J. Am. Chem. Soc*. **1994**, *116*, 5898.

(26) Malkin, V. G.; Malkina, O. L.; Salahub, D. R. *Chem. Phys. Lett*. **1993**, *204*, 80; **1993**, *204*, 87.

(27) Stewart, J. J. P. *J. Comput.-Aided Mol. Des*. **1990**, *4*, 1.

(28) Müller, K., manuscript in preparation .

(29) Schmider, J.; Müller, K. *J. Phys. Chem. A* **1998**, *102*, 1181.

(30) Wittebort, R. J.; Olejniczak, E. T.; Griffin, R. G. *J. Chem. Phys*. **1987**, *86* 5411.

(31) Redfield, A. G. *Adv. Magn. Reson*. **1965**, *1*, 1.

(32) Boeffel, C.; Luz, Z.; Poupko, R.; Vega, A. J. *Isr. J. Chem*. **1988**, *28*, 283.

(33) Schmidt-Rohr, K.; Spiess, H. W. *Multidimensional Solid-State NMR and Polymers*; Academic Press: London, 1994.

(34) Gelerinter, E.; Luz, Z.; Poupko, R.; Zimmermann, H. *J. Phys. Chem*. **1990**, *94*, 8845.

(35) Spiess, H. W.; Sillescu, H. *J. Magn. Reson*. **1982**, *42*, 381.

(36) Poupko, R.; Furman, E.; Müller, K.; Luz, Z. *J. Phys. Chem*. **1991**, *95*, 407.

(37) Liebelt, A.; Müller, K., manuscript in preparation.

(38) Wefing, S.; Kaufmann, S.; Spiess, H. W. *J. Chem. Phys*. **1988**, *89*, 1234.

(39) Müller, K. *J. Phys. Chem*. **1992**, *96*, 5733.

(40) Chatani, Y.; Anraku, H.; Taki, Y. *Mol. Cryst. Liq. Cryst*. **1978**, *48*, 219.

(41) Wittebort, R. J.; Szabo, A. *J. Chem. Phys*. **1978**, *69*, 1722.

(42) Torchia, D. A.; Szabo, A. *J. Magn. Reson*. **1982**, *42*, 107.